

# THERMAL SIMULATIONS OF WIRE PROFILE MONITORS IN ISIS EXTRACTED PROTON BEAMLINE 1

D. W. Posthuma de Boer\*, A. Pertica, ISIS, STFC, Rutherford Appleton Laboratory, Oxfordshire, OX11 0QX, UK

## Abstract

Wire scanners and secondary emission (SEM) grids are used for measurements of transverse beam profile at the ISIS neutron and muon source. Silicon carbide-coated carbon fibre wires are used in profile monitors throughout the ISIS accelerator. One such SEM grid is currently installed close to the target in Extracted Proton Beamline 2 (EPB2) and is intercepted by the 800 MeV proton beam at a repetition rate of 10 Hz. Future profile measurements will require another of these monitors to be installed close to the target in EPB1; intercepted with a repetition rate of 40 Hz.

Wires intercepting the ion beam are heated due to the deposition of beam-energy. Thermal simulations for the higher repetition rate were performed using ANSYS and a numerical code. The numerical code was then expanded to include various beam, wire and material properties. Assumptions for temperature dependent material emissivities and heat capacities were included in the simulation. Estimated temperatures due to the energy deposited by protons, and approximate values of deposited energy from the expected neutron flux are presented. The effects on wire-temperature of various beam and wire parameters are also discussed.

## INTRODUCTION

Intercepting wires are used at accelerator facilities around the world to measure transverse and longitudinal beam properties. Beam particles either knock electrons from the wire or deposit some charge, inducing a current which is proportional to the flux of the beam. By measuring the relative current at multiple transverse positions, a beam profile can be obtained [1].

The ISIS facility at the Rutherford Appleton Laboratory is a spallation neutron and muon source delivering an average of 0.2 MW of proton beam power to two target stations (TS1 & TS2). During acceleration and extraction wire-based monitors are used to measure the transverse beam profile. At ISIS the intercepting wires are silicon-carbide (SiC) coated carbon fibres with a diameter of 142  $\mu\text{m}$ .

A wire grid is currently installed in EPB2 close to the TS2 target, with the wires intercepting the beam at a rate of 10 Hz. Future profile measurements will require a second grid to be installed in EPB1 close to the TS1 target. These wires will intercept the 800 MeV proton pulses at a repetition rate of 40 Hz. Thermal simulations are required to verify that wires in EPB1 will be able to withstand temperatures resulting from this higher repetition rate.

\* david.posthuma-de-boer@stfc.ac.uk

## THEORY

### Charged Particles in Matter

Energetic charged particles passing through a medium interact electromagnetically with atomic electrons, depositing energy by ionising constituent atoms. For a singly charged particle with a velocity  $v = \beta c$ , energy  $E$  and relativistic factor  $\gamma$ , passing through a material with atomic number  $Z$  and number density  $n$ , the energy deposited into the material per unit particle path length  $x$ ; the stopping power  $S(E)$ , follows the Bethe-Bloch equation

$$S(E) = -\frac{dE}{dx} \approx \frac{4\pi\hbar^2\alpha^2nZ}{m_e\beta^2} \left[ \ln\left(\frac{2v^2\gamma^2m_e}{I_e}\right) - \beta^2 \right], \quad (1)$$

where  $\alpha$  is the fine structure constant,  $I_e$  is the effective ionisation potential,  $m_e$  is the electron mass,  $c$  is the speed of light and  $\hbar$  is the Dirac constant [2]. An example of this for 800 MeV protons travelling in a tungsten medium is shown in Fig. 1. As the protons travel through the medium they lose kinetic energy to atomic electrons, increasing the value of  $S(E)$  [2]. A sharp increase in the stopping power; known as the Bragg peak, is seen towards the end of the range.

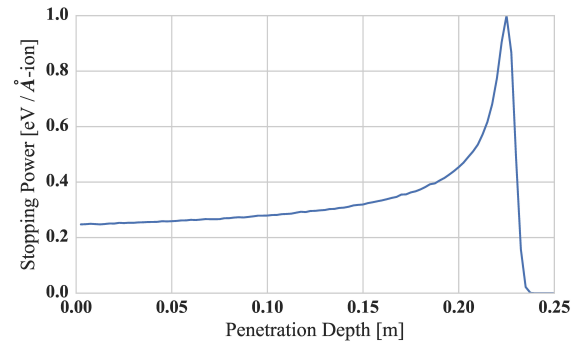


Figure 1: Results of a SRIM simulation showing the stopping power for 800 MeV protons in tungsten [3].

### Thermal Effects

From the definition of the constant-volume heat capacity it can be found that the change in temperature,  $\Delta T$ , of an object is given by:

$$\Delta T = \int \frac{1}{Mc_v} dU, \quad (2)$$

where  $U$  is the internal energy of an object,  $M$  is the energy-absorbing-mass and  $c_v$  is the constant-volume specific heat capacity of the material. Equation (2) shows that when energy is deposited into an object there is an associated increase in temperature [4].

Heat loss takes place by means of thermal conduction, convection and radiation. As profile monitor wires are thin and will be heated in vacuum, only radiation will be considered; the loss of energy by emission of photons. The total radiated power is given by the Stefan-Boltzmann law:

$$\dot{Q} = \epsilon \sigma A (T_1^4 - T_2^4), \quad (3)$$

where  $\dot{Q}$  is the heat energy,  $T_1$  is the temperature of the radiating object,  $T_2$  is the ambient temperature,  $\epsilon$  is the material emissivity,  $A$  is the materials surface area and  $\sigma$  is the Stefan-Boltzmann constant [4].

## SIMULATION

Simulating the heating of wires as they intercept the proton beam will require that a calculation be made for the energy deposited per proton. This is given by integrating  $S(E)$  over the proton's path through the wire. As a worst-case approximation all protons will be assumed to traverse the full wire diameter,  $d$  as indicated in Fig. 2; the largest direct path. Since the wire thickness is on the order of 100 µm and the range of 800 MeV protons in tungsten is approximately 20 cm; as shown in Fig. 1, the stopping power will be assumed to be constant. The energy deposited per proton was thus given by  $E_{\text{ion}} = S(E) \cdot d$ . Stopping powers were obtained from *PSTAR Tables* [5] and *SRIM* [3].

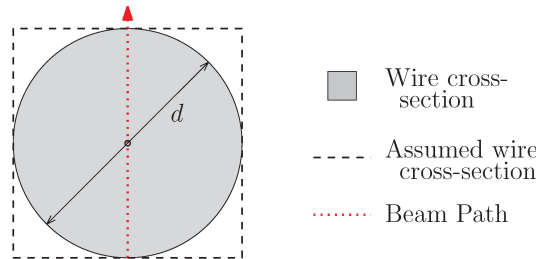


Figure 2: Assumed wire cross section in relation to physical dimensions; the assumed proton trajectory is also shown.

The assumed beam parameters are listed in Table 1. A frequency of 50 rather than 40 Hz will be used to calculate for the worst-case. Heating due to energy deposited by the beam will be calculated using Eq. (2). Cooling towards an ambient temperature of 300 K will be calculated using Eq. (3). Simulations were performed with ANSYS® 15.0 and a custom numerical code written in python.

Table 1: Assumed Beam Parameters at the End of EPB1

Parameter	Value
Beam $\sigma$	2.5 cm
Protons per bunch	$1.5 \times 10^{13}$
Bunch length	100 ns
Bunch spacing	250 ns
Bunches per pulse	2
Pulse frequency	50 Hz
Beam energy	800 MeV

## Material Properties

Equations (1), (2) and (3) show that the energy deposited into an object, the associated temperature increase as well as the radiated power each depend on the object's material properties. These properties are temperature dependent, and can vary due to manufacturing and finishing processes [6]. Material properties are often considered to be constant in such simulations [7], however in order to test the impact of temperature dependence, assumptions will be made for temperature dependent heat capacities and emissivities. The assumed emissivities for carbon fibres, SiC fibres and tungsten wires are shown in Fig. 3.

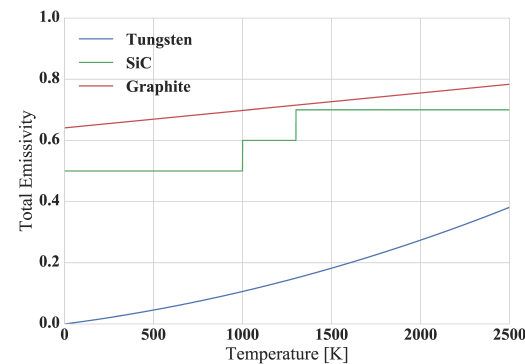


Figure 3: Assumed emissivities for simulated wire materials.

## RESULTS

### Comparison of Simulation Tools

Simulations of 30 µm diameter tungsten wires in a 181 MeV proton beam were initially run to compare predictions with previously published results, and to benchmark the two simulation techniques. Temperatures predicted by ANSYS® and the numerical code are shown in Fig. 4, where the temperature independent results appear to agree with those previously published; oscillating between around 3000 and 3500 K [8]. The simulations were then run with temperature dependent material properties. The two simulation methods were consistent, predicting maximum temperatures of approximately 1000 K lower than the temperature independent results (see Fig. 4).

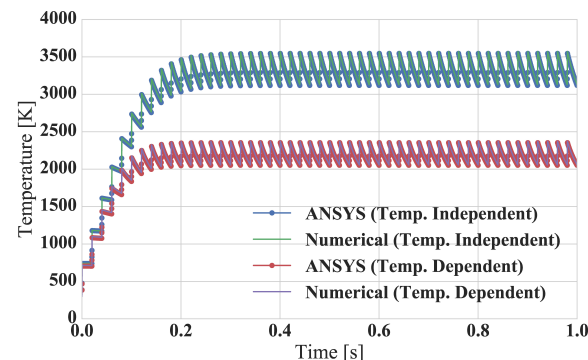


Figure 4: ANSYS® and numerical simulation results with constant and temperature dependent material properties.

## ISIS Beam Parameter Results

Numerical simulations were then run for the beam parameters shown in Table 1. One wire or beam property was varied for each simulation; each giving a result resembling Fig. 4. The maximum predicted wire temperature was then recorded and plotted against the variable parameter.

Tungsten wires were predicted to have the highest temperature for a given wire radius as shown in Fig. 5. Carbon fibres had the lowest predicted temperature due to their relatively low stopping power, and the comparatively high emissivity. No wires were predicted to exceed melting or sublimation temperatures [9, 10].

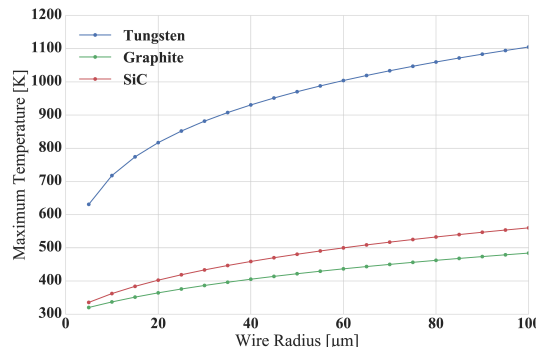


Figure 5: Variation of maximum temperature with intercepting wire radius; simulated with a numerical code.

Figure 6 shows the variation of maximum temperature with beam energy. The predicted variation in temperature over this energy range was 40, 20 and 25 K for tungsten, graphite and SiC respectively. Again no wires were predicted to exceed melting or sublimation temperatures.

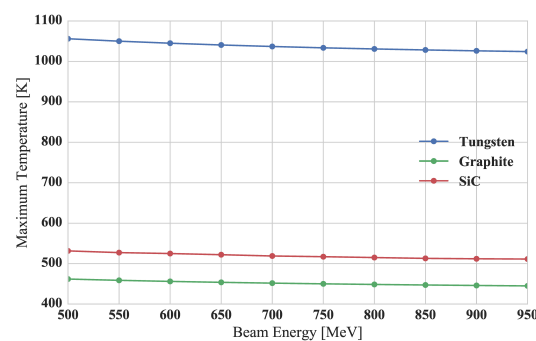


Figure 6: Variation of maximum temperature with incident proton beam energy; simulated with a numerical code.

## Neutron Flux Considerations

Due to the close proximity of the simulated wires to the TS1 target, neutrons originating from the target were also expected to deposit energy. The heating associated with this energy was also considered. A constant neutron production rate of  $2 \times 10^{16} \text{ s}^{-1}$  was assumed, distributed symmetrically over the surface of a sphere. The separation of the wires from the target was assumed to be 1 m, and the interception rate was found from the rectangular wire cross-section. It

was also assumed that  $3 \times 10^{10} \text{ cm}^{-2}$  neutrons provided a dose of 1 Gy [11]. This increased the simulated maximum temperature by less than 1% for all materials with the beam parameters shown in Table 1.

## CONCLUSION

Simulations of wire heating using ANSYS® and a numerical code were run with temperature independent material properties and found to agree with previously published results. The simulations were then modified to include approximate temperature dependent properties. This resulted in a reduction in predicted maximum temperature of approximately 1000 K. It should be noted that the assumptions made for material properties do not necessarily describe real wire materials and would ideally be measured experimentally.

Numerical simulations were then run for a near-target wire grid monitor with tungsten wires, carbon fibres and SiC coated carbon fibres. Maximum temperatures for different wire & beam properties were recorded with none of the simulated wires reaching melting or sublimation temperatures, even with a neutron flux contribution.

While heating due to secondary neutrons was considered, other secondary particles were neglected. A more complete analysis would additionally include the energy deposited by photons and other secondary particles from the target.

## REFERENCES

- [1] P. Strehl, *Beam Instrumentation and Diagnostics*. Springer Berlin Heidelberg, 2006.
- [2] M. Thomson, *Modern Particle Physics*, Cambridge University Press, 2013, pp. 10–14.
- [3] J. F. Ziegler *et al.*, "SRIM – The stopping and range of ions in matter (2010)", *Nucl. Instr. Meth. B*, vol. 268, Jun. 2010.
- [4] L. M. Jiji, *Heat Conduction*. Springer Berlin Heidelberg, 2009, pp. 11, 354.
- [5] Stopping-Power and Range Tables for Electrons, Protons, and Helium Ions, <http://physics.nist.gov/PhysRefData/Star/Text/contents.html>
- [6] D. Alfano *et al.*, "Emissivity and catalycity measurements on SiC-coated carbon fibre reinforced silicon carbide composite", *Journal of the European Ceramic Society*, vol. 29, pp. 2045–2051, Jan 2009.
- [7] T. Yang *et al.*, "Thermal analysis for wire scanners in the CSNS Linac", *Nucl. Instr. Meth. A*, vol. 760, pp. 10–18, Oct. 2014.
- [8] H. Akikawa *et al.*, "Wire Profile Monitors in J-PARC Linac", in *Proc. LINAC'06*, Knoxville, Tennessee, USA, Aug. 2006, paper TUP021, pp. 293–295.
- [9] D. R. Lide, 4-122 and 12-94, in *Handbook of Chemistry and Physics*, 79th Ed. CRC Press, 1998.
- [10] H. O. Pierson, *Handbook of Refractory Carbides and Nitrides*, William Andrew, 1996.
- [11] J. Gibson and E. Piesch, "Neutron Monitoring for Radiological Protection", IAEA, Vienna, 1985.